Levels of ^{141}Cs and ^{141}Ba from the decays of ^{141}Xe and ^{141}Cs

D. Otero, A. N. Proto, and F. C. Iglesias

Departamento de Física Nuclear, Comisión Nacional de Energía Atómica,
Av. Libertador 8250, Buenos Aires (29), Argentina

The γ rays and conversion electrons following the β decay of ^{141}Xe and ^{141}Cs have been measured by applying on-line mass-separation techniques to ^{235}U fission products. Internal-conversion coefficients were determined for 10 transitions, and level schemes for the two daughter nuclei, ^{141}Cs and ^{141}Ba, are proposed based on the study of γ-singles, $\gamma\gamma$-coincidence, and internal-conversion electron spectra.

> RADIOACTIVITY ^{141}Xe, ^{141}Cs; measured E_γ, I_γ, $\gamma\gamma$ coin, ICC; deduced logft;
> measured $T_{1/2}$ ^{141}Xe, ^{141}Cs; deduced levels. On-line measurements, mass-sep-
> arated ^{235}U fission products.

I. INTRODUCTION

In this paper our results are reported for the levels of ^{141}Cs and ^{141}Ba populated in the β^- decays of 1.7-sec ^{141}Xe and 24.0-sec ^{141}Cs. The activities were produced using on-line mass separation of uranium-fission products, followed by on-line measurements of γ rays and conversion electrons.

Previously, Alväger et al.[1] and Tamai et al.[2] had identified some of the stronger γ rays of the mass-141 chain. Recently, Talbert et al.[3] presented their preliminary results on γ-ray energies and intensities, and a level scheme (also preliminary) for ^{141}Cs (see Sec. IV A). Up to now no level scheme for ^{141}Ba has been proposed. Half-lives for both the ^{141}Xe and ^{141}Cs ground-state decays had been measured before, and the results are summarized in Ref. 4. In a recent study, Morman, Schick and Talbert[5] reported lifetimes of several levels in ^{141}Cs and ^{141}Ba (see Sec. V).

In the present work we propose for ^{141}Cs a level scheme of 38 levels connected by 166 transitions which carry 91% of the total observed γ intensity. For ^{141}Ba a level scheme of 27 levels containing 78 transitions which represent 65% of the observed γ intensity is proposed.

II. EXPERIMENTAL PROCEDURE

The mass-141 sources were obtained at the Buenos Aires on-line facility (IALE project) which has been described in Ref. 6. A target of uranyl-stearate, enriched to about 90% in ^{235}U, is placed in a thermal neutron flux of about 5×10^8 n cm^{-2} sec^{-1}; the rare gas fission products are continuously fed into the ion source of the mass

separator and the selected activity is collected on a moving aluminized Mylar tape collector.

Two Ge(Li) detectors of 35 and 45 cm^3 were used to measure the γ spectra; the resolution for the ^{60}Co γ rays was 2.2 and 2.8 keV, respectively. The data were recorded in an analyzer system provided with two 4096-channel analog-to-digital converters and several readout peripherals under control of a 16 000-memory computer. The recorded spectra were analyzed either by hand or by computer methods using the ANPIK program,[7] which can be operated on the above mentioned computer.

In order to assign transitions to either the 1.7-sec ^{141}Xe decay, or the 24.0-sec ^{141}Cs decay, an identification by means of the half-life differences was made using the moving-tape collector with appropriate cycling.[8]

The two Ge(Li) detectors mentioned were also used for the $\gamma\gamma$-coincidence measurements. The coincidence circuits were of the fast-slow type, with $2\tau \simeq 50$ nsec from 200 to 1500 keV, and a slow type with $2\tau \simeq 200$ nsec from 30 to 1500 keV.[9] The results in the overlapping energy region were similar. Coincidence events were stored as 4096 $\times$ 4096 bidimensional data. The signals were processed by two ADCs and both addresses generated stored on a magnetic-tape buffer. The data recorded on this tape were later read back into the computer through appropriate windows, subtracting coincidences due to background and Compton distributions.

Energy and efficiency calibrations were performed using the method described in Ref. 10. Ground-state half-lives were measured using the multiscaling technique.

The internal-conversion-coefficient determinations for transitions with energies above 100 keV was made by means of the NPG (normalized-K-conversion peak-to-γ peak method). The whole procedure is fully described in Ref. 11. In the present work we use a 3-cm^2 area, 3-mm depletion depth Si(Li) detector; the γ rays were measured with the above mentioned 2.2-keV resolution detector. In order to collect only the desired activity, either Xe or Cs, a moving tape collector for electrons was used, with appropriate cycling.

A Si(Li) x-ray detector of 290-eV resolution full width at half maximum at 5.9 keV was used for low-energy γ-ray measurements. Efficiency and energy calibrations were made as described in Ref. 12. An internal-conversion coefficient by means of the XPG (x-ray-peak-to-γ-peak method)[12] was also obtained from measurements with this detector, as well as the half-life for x-rays and a low-energy transition.

III. EXPERIMENTAL RESULTS

A. ^{141}Xe decay

In Fig. 1 a partial γ spectrum with enhanced ^{141}Xe activity is shown. The enhancement with respect to the ^{141}Cs activity was obtained by removing the collected activity every 8 sec. Singles-γ spectra in the energy region of 0 to 5 MeV were taken with the 2.2-keV resolution Ge(Li) detector. The averaged results from several runs of energy and intensity determinations are summarized in Table I. We were able to assign unambiguously 209 γ transitions to the ^{141}Xe decay. Our results

are in general agreement with the preliminary results of Talbert et al. in Ref. 3.

The $\gamma\gamma$-coincidence results are given in Table II and typical coincidence spectra are shown in Fig. 2. These spectra arise from recording coincidence events during 80 h.

The half-life for the ^{141}Xe ground-state decay was determined to be 1.72 ± 0.03 sec. This value was obtained as a weighted average of those of the 68.98-, 81.81-, 100.76-, 105.96-, and 118.71-keV transitions. Using the Si(Li) x-ray detector the half-life of the ^{141}Cs $K_{\alpha} + K_{\beta}$ lines was also measured giving a value of 1.7 ± 0.1 sec, thus ensuring that the γ rays which follow the 1.72-sec half-life belong to the ^{141}Xe decay. These results are in agreement with the adopted values of Ref. 4.

A special run was made to determine the β^- feeding to the ^{141}Cs ground state. The activity of the 141-mass chain was collected for about 10 hours; this means that the ^{141}Xe, ^{141}Cs, and ^{141}Ba activities were in equilibrium and only the ^{141}La activity had to be slightly corrected for half-life. The collection rate was kept constant by monitoring the activity at the mass-separator collector during the whole measurement through the rate of the 909.45-keV γ-ray transition. Through the 1354.52-keV transition of the ^{141}La decay, whose intensity in percent of β^- disintegrations is well known,[3] it is possible to establish: (a) the total number of β^- decays in the mass chain and (b) the intensity of the γ transitions belonging to the ^{141}Xe decay per unit of β^- disintegration. From the ^{141}Cs level scheme (see Sec. IV) we were able to determine the β^- feedings to excited levels of ^{141}Cs,
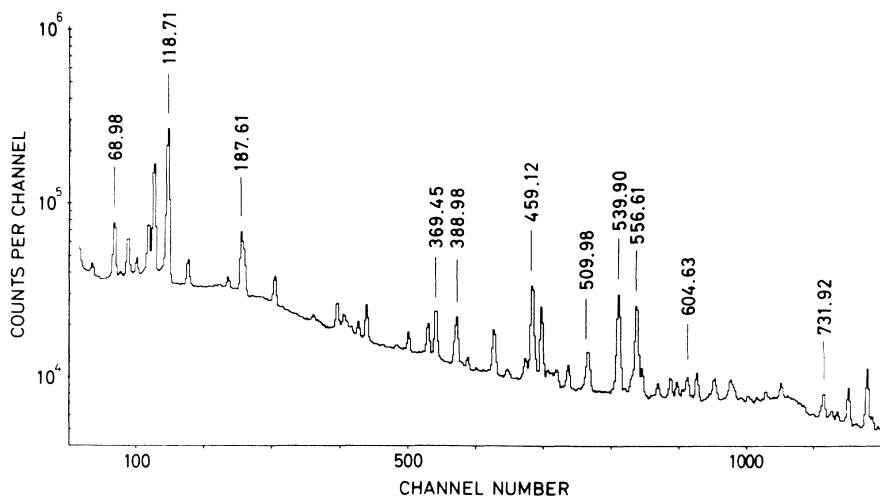

FIG. 1. Partial γ spectrum with enhanced Xe activity. Some of the Xe decay full-energy peaks are labeled with the corresponding energy value.

TABLE I. γ rays observed in the decay of ^{141}Xe.

Energy (keV)	Relative intensity [a]	Energy (keV)	Relative intensity [a]
68.98 ± 0.03	187.0 ± 30.0	729.01 ± 0.16	7.4 ± 0.6
81.81 ± 0.02	99.0 ± 13.0	731.92 ± 0.04	32.9 ± 1.1
89.74 ± 0.31	28.9 ± 3.2	737.38 ± 0.68	3.4 ± 0.7
93.73 [b] ± 0.35	0.8 ± 0.2	739.30 ± 0.13	3.9 ± 0.9
96.34 ± 0.23	3.8 ± 0.6	745.19 ± 0.10	9.5 ± 1.3
100.76 ± 0.03	110.0 ± 12.0	755.29 ± 0.03	52.4 ± 2.1
105.96 ± 0.03	367.0 ± 40.0	769.68 [c] ± 0.74	1.5 ± 0.5
118.71 ± 0.02	522.0 ± 58.0	773.08 ± 0.10	99.6 ± 4.3
137.68 ± 0.02	32.7 ± 3.4	778.01 ± 0.10	11.8 ± 3.0
149.40 [b] ± 0.05	4.3 ± 0.6	783.67 ± 0.29	4.5 ± 2.5
152.20 ± 0.95	1.0 ± 0.2	791.96 ± 0.12	14.9 ± 1.3
168.17 ± 0.19	1.3 ± 0.1	801.21 ± 0.59	6.2 ± 1.6
177.71 ± 0.33	1.4 ± 0.1	805.36 [b] ± 0.17	12.4 ± 1.2
187.61 ± 0.08	116.4 ± 5.3	807.31 ± 0.20	9.7 ± 1.3
234.61 ± 0.34	2.3 ± 0.2	818.59 ± 0.59	2.7 ± 0.8
244.40 ± 1.10	0.6 ± 0.2	823.37 [b] ± 0.13	9.4 ± 0.9
246.70 ± 1.10	0.8 ± 0.2	827.23 ± 0.57	4.4 ± 0.9
254.32 ± 0.25	5.4 ± 0.4	843.01 [b] ± 0.07	18.6 ± 1.4
280.30 ± 0.26	2.0 ± 1.0	854.74 [c] ± 0.12	11.1 ± 2.0
283.13 ± 0.04	18.1 ± 1.5	863.50 ± 0.79	1.2 ± 0.6
286.06 ± 0.05	9.9 ± 0.5	869.20 ± 0.65	13.0 ± 1.3
313.00 ± 2.0	1.0 ± 0.3	870.52 [b] ± 0.22	<4.0
314.79 ± 0.32	1.2 ± 0.2	874.61 ± 0.24	15.1 ± 2.6
317.60 [c] ± 0.74	0.9 ± 0.2	880.67 ± 0.35	3.6 ± 1.7
332.67 ± 0.23	3.5 ± 0.3	894.71 ± 0.16	36.2 ± 4.5
335.94 ± 0.25	2.4 ± 0.4	898.16 [b] ± 0.36	8.3 ± 2.1
362.02 ± 0.03	39.3 ± 7.0	909.45 ± 0.04	1000.0 ± 26.0
369.45 ± 0.05	72.3 ± 7.0	914.27 [c] ± 0.16	8.1 ± 0.8
388.98 ± 0.06	68.3 ± 5.3	933.51 ± 0.24	6.2 ± 0.8
422.13 ± 0.48	15.6 ± 2.4	942.75 [b] ± 0.41	11.3 ± 1.3
423.87 [b] ± 0.07	54.9 ± 4.1	943.56 ± 0.39	9.6 ± 1.6
433.25 ± 0.69	2.1 ± 0.3	944.79 ± 0.27	5.8 ± 1.4
434.85 ± 0.18	8.0 ± 1.5	976.63 [c] ± 0.63	5.5 ± 1.8
436.18 ± 0.42	3.0 ± 0.5	979.98 ± 0.09	44.7 ± 1.9
437.94 ± 0.31	3.9 ± 0.6	986.01 [b] ± 0.12	16.7 ± 1.0
450.98 ± 0.23	6.5 ± 0.8	989.55 ± 0.56	8.5 ± 0.9
452.65 ± 0.08	22.5 ± 0.8	991.65 ± 0.30	9.3 ± 1.4
459.12 ± 0.06	201.1 ± 15.0	998.73 ± 0.42	7.3 ± 1.1
467.80 ± 0.06	128.7 ± 8.0	1008.45 ± 0.41	19.0 ± 4.0
492.85 [b] ± 0.05	30.3 ± 1.4	1015.23 ± 0.14	14.9 ± 0.8
507.26 [b] ± 0.31	8.6 ± 1.6	1025.31 [b] ± 0.20	9.9 ± 0.9
509.98 ± 0.08	34.7 ± 1.4	1028.13 ± 0.03	76.3 ± 8.6
532.34 ± 0.35	2.6 ± 0.5	1051.88 ± 0.08	46.7 ± 1.8
538.01 [c] ± 0.18	29.3 ± 5.0	1062.48 ± 0.22	8.5 ± 1.4
539.90 ± 0.09	235.0 ± 13.0	1090.60 ± 0.56	10.0 ± 0.8
551.68 [b] ± 0.10	20.9 ± 2.2	1092.82 ± 0.26	8.5 ± 1.1
556.61 ± 0.15	212.0 ± 42.0	1097.19 ± 0.25	19.9 ± 4.3
569.74 ± 0.56	4.1 ± 0.7	1099.68 [b] ± 0.47	20.0 ± 11.0
576.77 ± 0.11	16.2 ± 1.0	1104.88 ± 0.27	7.2 ± 1.1
578.19 [b] ± 0.21	5.7 ± 0.6	1112.33 ± 0.42	4.8 ± 1.2
594.33 ± 0.17	16.8 ± 1.2	1120.98 ± 0.06	32.7 ± 1.1
599.61 ± 0.13	5.8 ± 1.0	1131.30 [b] ± 0.28	3.8 ± 1.1
604.63 [b] ± 0.26	10.5 ± 2.0	1134.56 [b] ± 0.16	13.6 ± 1.1
613.17 [b] ± 0.07	36.7 ± 5.5	1140.41 [b] ± 0.14	5.0 ± 1.2
629.50 ± 0.20	21.7 ± 1.0	1177.68 ± 0.20	6.6 ± 1.2
644.36 ± 0.11	30.0 ± 2.1	1196.67 ± 0.40	8.5 ± 2.4
649.23 [b] ± 0.22	10.7 ± 1.9	1204.89 ± 0.69	2.2 ± 0.8
677.85 [d] ± 0.10	11.1 ± 3.2	1208.10 ± 0.49	6.2 ± 0.7
722.13 [b] ± 0.35	3.3 ± 0.9	1214.54 [b] ± 0.08	12.7 ± 1.7

TABLE I *(Continued)*

Energy (keV)	Relative intensity [a]	Energy (keV)	Relative intensity [a]
1217.48 ±0.12	20.0± 1.1	1917.84 ±0.26	7.6± 1.2
1219.50 ±0.37	7.1± 0.8	1921.72 ±0.35	3.8± 1.1
1233.02 [b] ±0.44	8.0± 1.4	1933.93 [b] ±0.32	8.3± 1.3
1246.17 [b] ±0.11	13.0± 1.3	1960.55 ±0.70	3.5± 0.7
1253.13 ±0.25	9.4± 2.3	2016.32 [b] ±0.49	8.8± 1.3
1275.47 ±0.69	2.8± 0.9	2020.27 ±0.21	9.2± 1.1
1310.69 ±0.43	5.8± 0.8	2058.13 ±0.29	5.9± 1.2
1317.82 ±0.94	5.4± 1.2	2109.34 ±0.36	5.5± 1.1
1323.94 [b] ±0.14	5.7± 1.5	2125.56 ±0.87	3.7± 1.1
1330.04 ±0.49	4.6± 1.2	2142.42 [c] ±0.21	3.6± 1.1
1351.72 ±0.16	10.5± 1.8	2168.73 ±0.54	2.8± 1.1
1360.21 [c] ±0.21	4.5± 1.0	2172.76 ±0.59	5.6± 1.2
1369.20 ±0.09	35.0± 1.1	2210.39 [b] ±0.24	7.6± 0.8
1372.10 ±0.21	8.1± 1.0	2217.31 ±0.73	8.1± 1.0
1386.93 ±0.23	5.9± 0.7	2231.46 ±0.51	4.4± 1.0
1393.34 [b] ±0.38	4.3± 0.8	2236.62 ±0.33	5.3± 1.0
1401.50 ±0.79	1.8± 0.8	2268.93 ±0.34	4.5± 1.2
1407.37 ±0.78	2.6± 1.1	2282.68 ±0.39	7.1± 0.8
1413.24 ±0.39	4.1± 1.2	2288.40 ±1.20	3.8± 0.8
1421.18 [b] ±0.86	2.3± 0.9	2336.57 [b] ± 0.54	4.0± 1.0
1428.21 ±0.57	3.5± 1.0	2371.83 ±0.50	2.5± 0.7
1436.25 ±0.10	25.9± 8.5	2394.23 [b] ±0.31	10.2± 1.3
1439.48 [b] ±0.45	7.9± 1.8	2410.60 ±0.29	5.7± 0.7
1489.13 ±0.16	10.8± 1.2	2430.08 ±0.39	5.6± 1.0
1497.93 ±0.32	4.9± 0.9	2448.76 [b] ±0.72	3.1± 0.8
1502.37 ±0.19	17.1± 1.3	2476.40 ±0.64	3.0± 0.7
1510.76 ±0.38	4.0± 0.8	2487.75 [c] ±0.57	2.7± 0.7
1526.63 ±0.47	5.5± 1.6	2547.17 ±0.23	17.5± 1.3
1539.56 ±0.70	5.1± 1.5	2577.17 ±0.81	5.0± 1.0
1546.89 ±0.29	5.4± 0.8	2601.13 ±0.66	6.9± 1.1
1550.96 [b] ±0.37	6.6± 1.2	2629.51 ±0.59	4.7± 1.1
1556.96 ±0.16	131.2± 9.6	2635.23 ±0.55	4.9± 1.1
1579.37 ±0.39	6.0± 1.1	2665.23 ±0.48	3.7± 0.7
1600.93 ±0.29	5.8± 0.7	2682.32 ±0.36	4.9± 1.2
1620.42 ±0.71	3.1± 1.1	2709.57 [c] ±0.23	5.4± 0.9
1655.41 ±0.75	6.6± 1.2	2734.19 ±0.39	6.4± 1.6
1688.12 [b] ±0.16	11.8± 1.0	2791.39 ±0.47	1.5± 0.9
1738.78 ±0.51	5.7± 2.1	2827.21 ±0.59	3.7± 0.9
1748.89 [b] ±0.33	4.8± 1.4	2839.24 ±0.67	5.1± 0.7
1755.58 [b] ±0.12	24.1± 1.5	2874.99 ±0.39	3.9± 0.7
1769.99 [b] ±0.21	17.4± 1.3	2896.73 [c] ±0.73	2.1± 0.6
1795.24 ±0.72	6.6± 1.0	2910.26 ±0.45	1.8± 0.7
1799.79 ±0.18	13.0± 1.0	2945.52 [c] ±1.18	2.8± 1.5
1829.47 ±0.31	6.7± 0.9	2984.81 ±0.85	2.3± 0.8
1860.54 ±0.14	9.5± 0.9	3103.02 ±0.61	3.2± 0.8
1882.02 ±0.53	5.6± 1.4	3221.51 ±0.73	2.2± 0.5
1898.47 ±0.95	6.2± 1.5		

[a] The error stated for the intensity normalized to 1000 has not been included in the errors of the other intensities.
[b] Not placed in the level scheme.
[c] Placed twice in the level scheme.
[d] Placed three times in the level scheme.

and, consequently, from (a) we obtained a value of $(49 \pm 5)\%$ for the β^- branch to the ^{141}Cs ground state.

Figure 3 shows an on-line electron spectrum of the decay of ^{141}Xe. The K-conversion coefficients were all obtained through the NPG method (see Sec. II) and are collected in Table III. We assigned the proposed multipolarities by comparing

TABLE II. γ-γ coincidence results for the ^{141}Xe decay.

Gate transitions (keV)	Coincidence transitions (keV)
69.0	118.7, 459.1, 369.5(?), 539.9(?), 909.5
81.8	106.0, 459.1, 909.5
89.7	362.0(?), 422.1-423.9(?), 467.8, 539.9
100.8	106.0, 773.1, 1028.1(?)
106.0	81.8, 100.8, 362.0, 459.1(?), 538.0-539.9, 773.1(?), 909.5
118.7	69.0, 369.5, 459.1, 539.9, 792.0(?), 909.5, 1369.2(?)
137.7	69.0, 773.1
187.6	369.5(?), 459.1, 909.5, 1369.2(?)
283.1	755.3(?)
362.0	106.0
369.5	118.7, 187.6, 539.9
389.0	556.6
422.1-423.9	369.5(?), 556.6(?), 909.5(?)
459.1	69.0(?), 81.8(?), 106.0(?), 118.7, 187.6, 539.9, 556.6, 909.5
467.8	89.7, 510.0
510.0	467.8
538.0-539.9	106.0, 118.7, 369.5, 459.1, 556.6
556.6	389.0(?), 459.1(?), 539.9
755.3	100.8(?), 106.9(?), 283.1(?)
773.1	69.0(?), 100.8, 106.0, 137.7
909.5	69.0(?), 81.8, 106.0, 118.7, 187.6, 459.1
1028.1	100.8(?)
1369.2	187.6(?), 118.7(?)
1557.0	...

our experimental values with the theoretical ones given in Ref. 13.

B. ^{141}Cs decay

A typical partial γ-ray spectrum taken with the ^{141}Cs activity enhanced with respect to the ^{141}Xe one is shown in Fig. 4. It is the result of the sum of about two-thousand spectra, each recorded during 1 min after switching off the separator beam and waiting a period of 10 sec. The energies and relative intensities of the γ rays assigned to the ^{141}Cs decay are listed in Table IV, and they are averaged results from several runs of energy and intensity determinations. The agreement with the preliminary results of Ref. 3 is only partial.

Table V contains the results of our $\gamma\gamma$-coincidence measurements. Since the coincidences were recorded simultaneously for ^{141}Xe and ^{141}Cs with their activities at saturation, the fact that 69.9% of ^{141}Cs decays proceed to the ^{141}Ba first excited level of 48.48 keV (Sec. IV B) limited our results to the dominant cascades in this nucleus.

A value of 24.94±0.06 sec was found for the ^{141}Cs ground-state decay, through the half-lives for the 48.48-, 554.74-, 561.51-, and 588.55-keV

γ rays. The half-lives of the $K_\alpha + K_\beta$ lines of ^{141}Ba were also measured in order to ensure the assignment in Z, giving a value of 24.9±0.7 sec. These results are in agreement with the adopted value of Ref. 4.

For the intensity of the β^- branch to the ^{141}Ba ground state we obtained a value of <5.9 per hundred disintegrations, using the same procedure as for the ^{141}Cs ground-state feeding and considering a pure $M1$ multipolarity for the 48.48-keV transition (see below).

The internal-conversion coefficient for the 48.48-keV transition was determined by the XPG method (Sec. II) and a value of $\alpha_K = 6.6 \pm 0.9$ was found.

Since theoretical α_K values for $M1$ and $E2$ multipolarities are covered by the experimental error of the measured α_K, the amount of $E2$ admixture cannot be obtained in this way. However, it is possible to calculate an upper limit for the $E2$ admixture if we use the level scheme proposed below. For the $M1$ and $E2$ multipolarities the theoretical total-conversion-coefficient values are (see Ref. 13) 7.7 and 18.2, respectively. From the ground-state intensity balance, the total-conversion coefficient for the 48.48-keV transition is <8.5, and thus we can establish an $M1$ (<9% $E2$) multipolarity for this low-energy transition. The maximum value for the $E2$ admixture corresponds to zero β feeding to the ground state. The limit for the lifetime of the 48.48-keV γ-ray transition established in Ref. 5 is in accordance with the systematics shown by Gove[14] for the $M1$ transitions.

From our electron spectra for ^{141}Cs we can conclude that the γ-ray (initial and final levels in parentheses) of 554.74 (1748.92-1194.16), 561.51 (561.51-0), 588.55 (588.55-0), 648.76 (2398.19-1748.92), and 691.93 (691.93-0) keV, which are the most intense in the decay of ^{141}Cs, have multipolarities lower than $E2$. This implies a $E1$-$M1$-$E2$ assignment.

IV. LEVEL SCHEMES

The level schemes we propose for ^{141}Cs and ^{141}Ba were constructed using the experimental results reported in Sec. III. The asterisks in Figs. 5(a)-5(c) and 6(a) and 6(b) identify the γ rays which fit twice in the level schemes; all of them were placed on the basis of energy sums and intensity balance considerations.

The logft values were calculated[15] taking into account for each level the balances of our intensities per hundred decays, our results for the half-lives of the decays as reported in Sec. III, and the Q_β values published in Ref. 16 for the
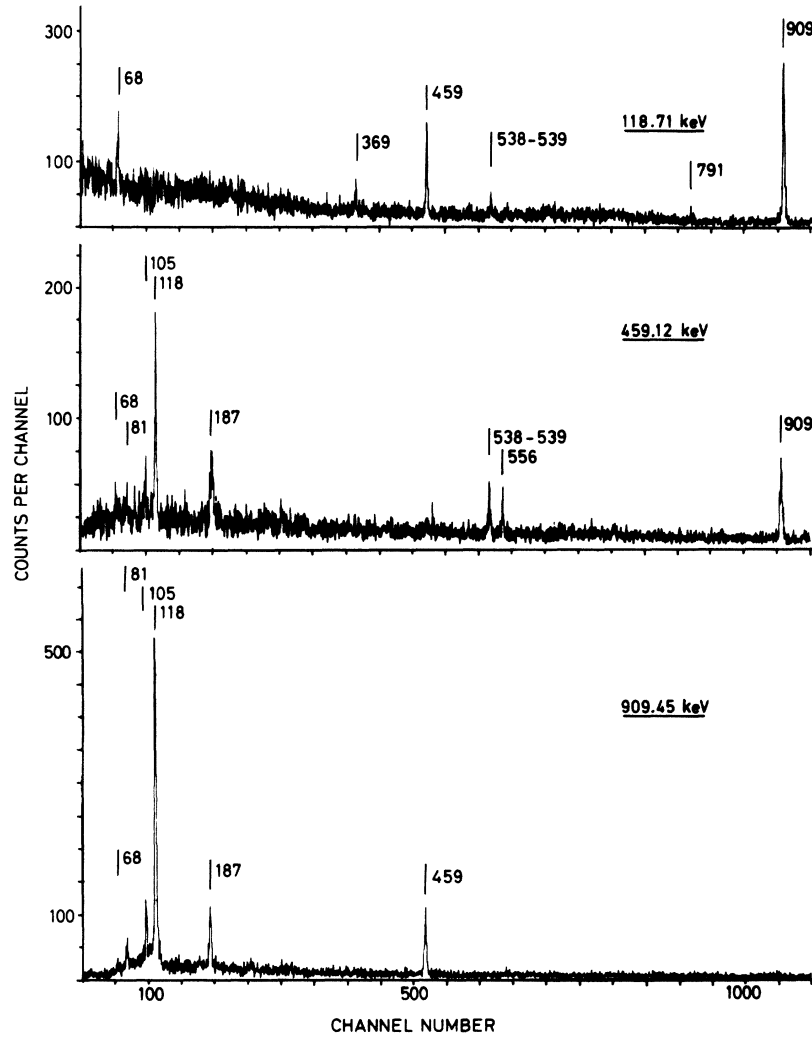
FIG. 2. Representative $\gamma\gamma$-coincidence spectra with: (a) 118.71-keV γ ray in gate, (b) 459.12-keV γ ray in gate, and (c) 909.45-keV γ ray in gate.
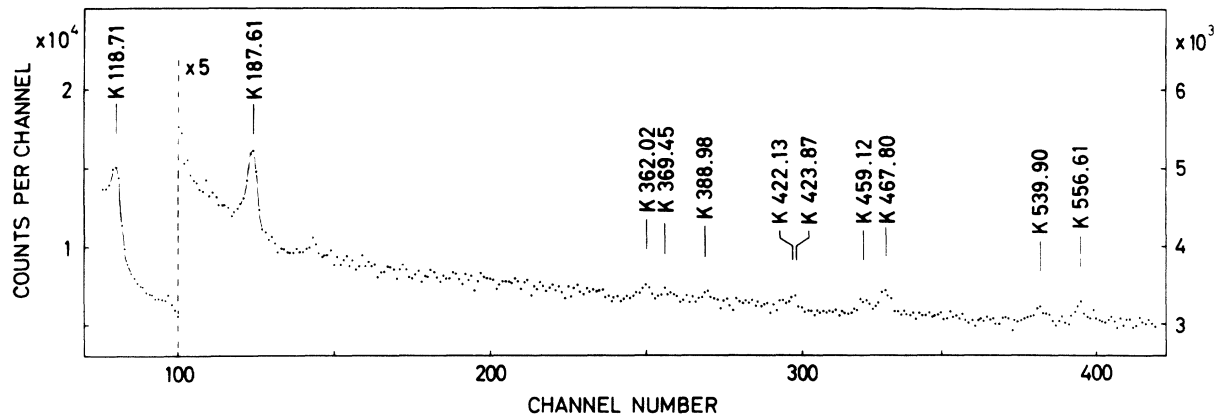

FIG. 3. On-line conversion-electron spectrum of the decay of ^{141}Xe, recorded with a Si(Li) detector during 20 hours. The on-line resolution of the detector in these measurements was about 7 keV at 200 keV.

TABLE III. K-conversion coefficients for ^{141}Xe decay.

Transition energy (keV)	α_K	Multipolarity assignment
118.5	0.200 ± 0.080	$M1\text{-}E2$
187.6	0.160 ± 0.060	$M1\text{-}E2$
362.0	0.024 ± 0.015	$M1\text{-}E2$
369.5	≤ 0.023	$E1\text{-}M1\text{-}E2$
389.0	0.020 ± 0.010	$M1\text{-}E2$
459.1	0.013 ± 0.006	$M1\text{-}E2$
467.8	0.015 ± 0.006	$M1\text{-}E2$
539.9	0.011 ± 0.003	$M1$ ($\leq 40\%$ $E2$)
556.6	0.008 ± 0.003	$M1\text{-}E2$

^{141}Xe decay and in Refs. 16 and 17 for the ^{141}Cs decay.

A. Scheme for ^{141}Cs

The level scheme proposed for ^{141}Cs is shown in Fig. 5. It contains 166 transitions (91% of the total observed γ intensity) within a frame of 38 levels. The levels established by $\gamma\gamma$ coincidence, energy sums, and intensity balances are 68.98, 105.96, 187.72, 206.69, 467.93, 557.10, 644.25, 946.01, 961.98, 977.53, 979.86, 1097.26, 1234.82, 1245.11, 1518.28, and 1556.71 keV. Into this set of 16 levels, we can place 72% of the total observed γ intensity.

The remaining levels are constructed only on the basis of energy combinations and intensity balances. All of them are connected to other levels by at least six transitions, except the levels at 4298.30 and 4793.67 defined by four and five transitions, respectively.

Log ft values have been calculated considering a Q_β value of 6.0 ± 0.1 MeV (Ref. 16) and assuming multipolarities lower than $E2$ for the γ-ray transitions whose energies were below 100 keV.

Recently, Morman et $al.$[5] have published the low-energy part of the level scheme of ^{141}Cs, which is a partial reproduction of that proposed in Ref. 3. From the eight levels proposed by these authors we have not confirmed those at 492.8 and 646.8 keV. Our experimental results did not show evidence enough as to establish a level at 492.8 keV, and for the transitions that Morman et $al.$ used in support of the 646.8-keV level, we were able to establish from our coincidence results that the 89.74-keV γ ray is placed between the levels at 467.93 and 557.10 keV (see Fig. 2 and Table II) and that the 459.93-keV transition connects the levels at 1097.26 and 1556.71 keV, thus leaving this presumed level unsupported.
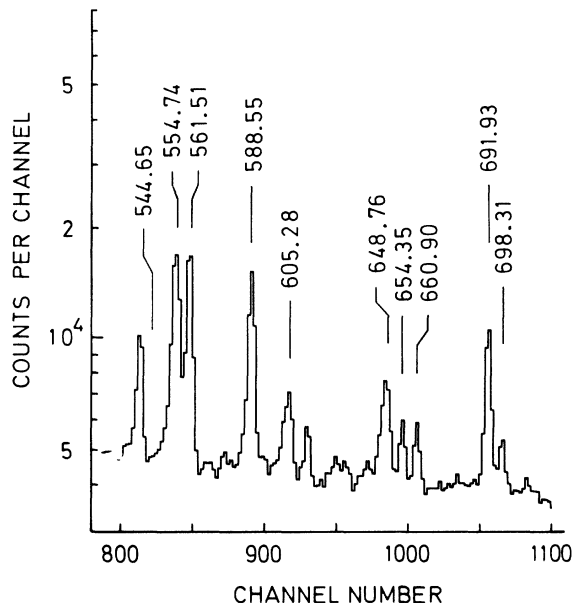

FIG. 4. Partial γ spectrum with enhanced Cs activity. This energy zone was chosen, as it contains the more intense transitions following the ^{141}Cs decay, except that of 48.48 keV (See Table IV).

B. Scheme for ^{141}Ba

The level scheme we proposed is shown in Figs. 6(a) and 6(b). It contains 78 transitions in a frame of 27 levels. The levels at 588.55, 1194.16, and 1748.92 keV are supported by γ-γ coincidences, as well as energy sums and intensity balances.

The levels at 48.48, 561.51, 691.93, and 1147.08 keV are postulated taking into account the lack of coincidence results with the crossover transitions, their relative intensity, and sum relations. The case of the 48.48-keV γ ray is the clearest, as this transition has an intensity of 69.9 per hundred decays.

The remainder of the levels are built using only energy sums and intensity balances. These levels are connected to other levels by at least six transitions, except the levels at 4040.22 and 4241.20 keV defined by four and five transitions, respectively.

The log ft values have been calculated taking into account the transition-intensity balance for each level, the β^- branch to the ground state, and the Q_β value which has been assumed to be 4.97 ± 0.07 MeV. This value arises from the weighted average between the results obtained in Refs. 16 and 17.

V. CONCLUSIONS

In the ^{141}Cs level scheme 72% of the total observed γ-ray intensity is accounted for by the 16

TABLE IV. γ rays observed in the decay of ^{141}Cs.

Energy (keV)	Relative intensity [a]	Energy (keV)	Relative intensity [a]
48.48 ± 0.03	1000.0 ± 180.0	1177.43 [b] ± 0.24	80.0 ± 13.0
206.53 [b] ± 0.13	19.2 ± 2.1	1182.42 [b] ± 0.24	25.3 ± 5.9
225.46 ± 0.17	3.0 ± 3.0	1191.27 ± 0.24	36.0 ± 16.0
242.33 ± 0.30	4.2 ± 1.8	1194.18 ± 0.06	425.0 ± 29.0
310.74 ± 0.38	5.3 ± 2.0	1226.37 ± 0.63	50.4 ± 4.2
325.48 ± 0.26	5.7 ± 3.8	1232.19 ± 0.68	11.8 ± 4.1
375.66 ± 0.66	4.5 ± 0.9	1253.10 ± 0.39	25.1 ± 2.7
385.10 ± 1.10	7.8 ± 3.7	1272.30 ± 0.17	14.3 ± 2.4
393.61 ± 0.20	27.0 ± 5.0	1277.90 ± 1.10	5.7 ± 3.4
416.99 [b] ± 0.19	30.0 ± 2.1	1290.84 [b] ± 0.69	40.0 ± 26.0
429.12 [b] ± 0.42	8.1 ± 1.8	1413.24 ± 0.39	13.8 ± 4.1
448.08 [c] ± 0.34	8.6 ± 1.3	1432.03 [b] ± 0.21	41.6 ± 3.5
497.33 ± 0.51	7.0 ± 2.0	1439.85 ± 0.72	13.7 ± 4.8
498.77 [b] ± 0.09	21.6 ± 2.7	1449.07 ± 0.14	34.7 ± 2.9
507.43 ± 0.31	32.3 ± 3.4	1497.76 ± 0.19	15.1 ± 3.4
512.52 [b] ± 0.17	33.0 ± 20.0	1518.10 ± 0.27	37.0 ± 10.0
544.65 [b] ± 0.27	20.5 ± 5.5	1606.35 ± 0.58	10.0 ± 2.0
554.74 ± 0.08	480.0 ± 39.0	1630.53 ± 0.31	18.6 ± 4.5
561.51 ± 0.03	550.0 ± 19.0	1661.22 ± 0.14	39.6 ± 3.4
585.45 ± 0.14	36.8 ± 4.5	1714.36 [b] ± 0.81	46.1 ± 4.1
588.55 ± 0.04	476.0 ± 24.0	1783.19 ± 0.32	13.4 ± 2.4
605.28 ± 0.24	73.8 ± 5.5	1789.55 ± 0.16	33.0 ± 3.1
639.03 [b] ± 0.17	31.1 ± 3.9	1809.30 ± 0.65	10.5 ± 3.4
648.76 ± 0.38	182.0 ± 29.0	1819.88 ± 0.20	33.9 ± 3.7
654.35 ± 0.09	84.0 ± 6.8	1825.56 [b] ± 0.26	13.4 ± 3.2
660.90 ± 0.07	91.4 ± 5.6	1860.59 [b] ± 0.15	19.2 ± 3.7
683.10 ± 1.40	8.1 ± 3.5	1871.09 [b] ± 0.54	15.2 ± 3.3
691.93 ± 0.04	380.4 ± 45.0	1876.77 ± 0.52	14.9 ± 5.4
698.31 [b] ± 0.08	51.8 ± 14.0	1883.13 ± 0.38	25.0 ± 5.0
717.56 ± 0.33	8.3 ± 1.7	1888.66 [b] ± 0.66	19.1 ± 3.4
724.20 ± 1.40	8.8 ± 4.0	1893.45 ± 0.18	45.6 ± 6.6
765.40 ± 0.51	8.1 ± 4.3	1906.13 ± 0.19	29.5 ± 4.3
778.00 [b] ± 0.11	45.8 ± 20.0	1918.04 [b] ± 0.19	25.5 ± 3.9
783.59 ± 0.26	10.0 ± 5.0	1922.02 [c] ± 0.35	8.6 ± 2.8
803.49 ± 0.23	50.0 ± 7.1	1933.53 [b] ± 0.24	19.7 ± 3.6
805.94 [b] ± 0.19	27.2 ± 3.8	1940.67 [b] ± 0.17	41.1 ± 4.7
811.99 ± 0.28	6.0 ± 3.0	1954.88 [b] ± 0.36	13.0 ± 2.3
827.04 ± 0.22	15.0 ± 7.0	1965.18 [b] ± 0.62	15.4 ± 2.1
933.12 [b] ± 0.25	10.0 ± 7.0	1989.63 [b] ± 0.34	16.4 ± 3.7
938.83 [b] ± 0.22	20.5 ± 2.5	1993.84 [b] ± 0.23	28.8 ± 3.2
948.01 ± 0.60	20.1 ± 3.0	1998.34 ± 0.29	28.8 ± 3.3
973.31 [b] ± 0.22	45.0 ± 13.0	2010.62 ± 0.70	7.4 ± 2.6
1008.10 [b] ± 0.73	41.2 ± 3.8	2045.25 ± 0.36	26.0 ± 4.1
1017.54 [b] ± 0.39	18.3 ± 8.7	2049.92 [b] ± 0.47	21.4 ± 6.8
1056.08 [b] ± 0.23	41.5 ± 7.4	2058.20 [b] ± 0.23	39.6 ± 4.7
1062.24 ± 0.23	81.0 ± 28.0	2064.74 [b] ± 0.20	18.2 ± 3.5
1067.92 [b] ± 0.11	43.5 ± 7.5	2087.91 ± 0.16	35.2 ± 4.7
1072.43 [b] ± 0.19	36.7 ± 4.3	2093.61 [b] ± 0.70	38.0 ± 5.1
1088.88 ± 0.49	20.0 ± 4.6	2142.48 [b] ± 0.23	15.5 ± 3.6
1110.37 [d] ± 0.27	31.5 ± 6.4	2184.34 ± 0.57	12.0 ± 3.1
1112.42 [b] ± 0.33	12.9 ± 2.7	2269.04 [b] ± 0.36	13.6 ± 2.5
1125.21 ± 0.83	8.0 ± 4.0	2303.39 [b] ± 0.82	46.3 ± 5.0
1131.04 [b] ± 0.42	12.0 ± 4.3	2326.57 [b] ± 0.46	12.9 ± 3.6
1140.60 [b] ± 0.08	89.0 ± 16.0	2338.51 [b] ± 0.80	10.7 ± 2.8
1147.08 ± 0.04	310.0 ± 14.0	2347.19 [b] ± 0.51	10.1 ± 2.2
1153.54 [b] ± 0.11	80.0 ± 7.9	2386.77 [b] ± 0.42	22.2 ± 4.7
1166.37 [b] ± 0.20	28.0 ± 3.7	2526.24 ± 0.39	16.6 ± 3.0
1168.59 ± 0.23	17.7 ± 3.8	2561.48 [c] ± 0.64	19.6 ± 5.7
1171.64 ± 0.06	88.0 ± 51.0	2624.42 ± 0.86	10.0 ± 3.0

TABLE IV *(Continued)*

Energy (keV)	Relative intensity [a]	Energy (keV)	Relative intensity [a]
2671.99 ± 0.51	9.7± 2.1	3115.60[b] ± 0.77	23.6± 6.4
2734.35[b] ± 0.22	14.8± 4.0	3133.44 ± 0.14	29.4± 6.1
2819.53[b] ± 0.21	36.0± 6.2	3193.12 ± 0.46	27.7± 4.4
2846.62 ± 0.35	19.6± 3.5	3205.17 ± 0.69	9.1± 3.1
2949.14[b] ± 0.24	29.4± 5.1	3224.79[b] ± 0.48	11.1± 3.0
2960.11[b] ± 0.46	12.9± 2.0	3228.74 ± 1.61	3.4± 2.0
2976.84 ± 0.46	10.3± 1.9	3252.39[b] ± 0.42	15.4± 6.1
2986.75 ± 0.66	8.0± 1.9	3259.54 ± 0.23	17.3± 9.9
3039.38 ± 0.65	23.0± 3.9	3330.90 ± 0.39	14.6± 4.1
3056.91[b] ± 0.47	17.9± 2.9	3348.29 ± 0.42	8.3± 1.6
3071.82[c] ± 0.27	45.8± 1.9	3379.37[c] ± 0.64	6.5± 1.9
3077.78 ± 0.37	26.4± 4.6		

[a] The error stated for the intensity normalized to 1000 has not been included in the errors of the other intensities.
[b] Not placed in the level scheme.
[c] Placed twice in the level scheme.
[d] Placed three times in the level scheme.

levels established by coincidences, which allows us to say that the main features of this level scheme are determined unambiguously.

None of the methods used in this work to obtain internal-conversion coefficients allowed the determination of those corresponding to the low-energy transitions (initial and final levels in parentheses) of 68.98 (68.98–0), 81.81 (187.61–105.96), 89.74 (557.10–467.93), 100.76 (206.69–105.96), and 105.96 (105.96–0) keV. For the case of the NPG method the efficiency of the detector was too small below about 80 keV, allowing the determination of the internal conversion at 118.71 keV as the lowest-energy transition. The XPG was not usable because of the great number of low-energy γ rays. However, taking into account the coinci-

TABLE V. γ-γ coincidence results for ^{141}Cs decay.

Gate transition (keV)	Coincidence transitions (keV)
48.5	No coincidence
554.7	648.8
588.6	554.7, 605.3
605.3	588.6
648.8	554.7, 561.5, 588.6

dence results, the above mentioned five low-energy transitions cannot have multipolarities higher than $M1$, $E2$, a result which agrees with the intensity balance of the levels involved. Consequently it was not possible to determine the β feeding to the levels at 68.98, 105.96, 188.16, and 206.69 keV. Due to the above mentioned limit on internal-conversion coefficients, however, the remainder of the β feedings could be calculated, since the uncertainty in the balance for the levels discussed above contributes but little to the over-all β-feeding balance.

In view of our disagreement with the scheme adopted by Morman et al.,[5] the limit of <2.4 nsec for the half-life for the proposed level at 646.8 keV should in fact belong to our level at 557.04 keV.

As regards the proposed scheme for ^{141}Ba, it is seen that its more relevant characteristic is the existence of a 48.48-keV transition which carries an intensity of 69.9 per hundred decays and depopulates the first excited level. Although in Table IV many unplaced γ rays are quoted, the intensity of all of them only represents about 12% of the total intensity of the transitions observed, when we take into account the conversion of 48.48-keV γ ray.

From the work of Morman et al., the upper limit for the half-life of the 48.48-keV first-excited level would be 3.4 nsec.
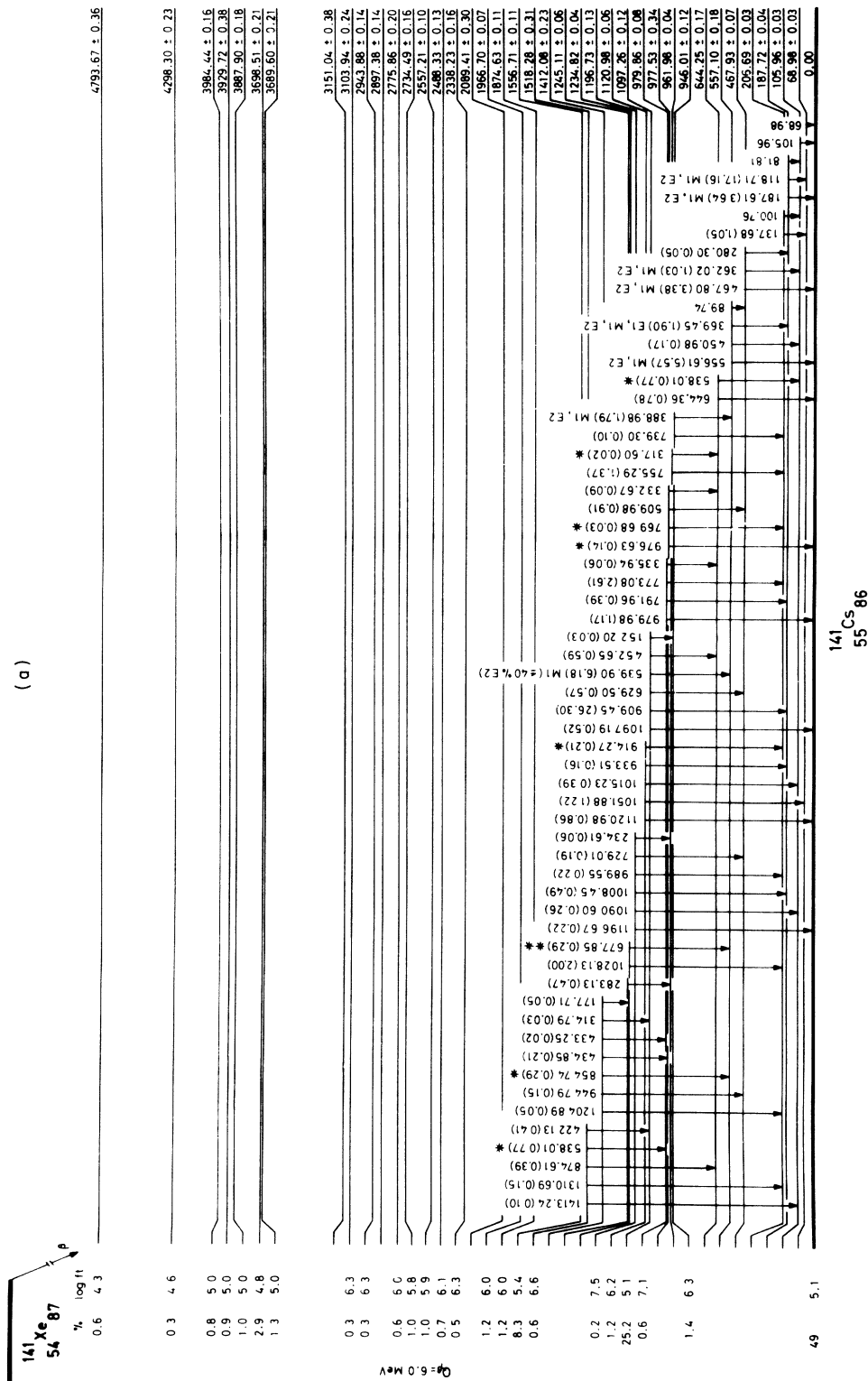
(a)

FIG. 5. (a) Low-energy part level scheme for ^{141}Cs. Transition intensities per 100 disintegrations are given in parentheses. Doubly placed γ rays are marked with asterisks. (b) Intermediate-energy part level scheme for ^{141}Cs. Transition intensities per 100 disintegrations are given in parentheses. Doubly placed γ rays are marked with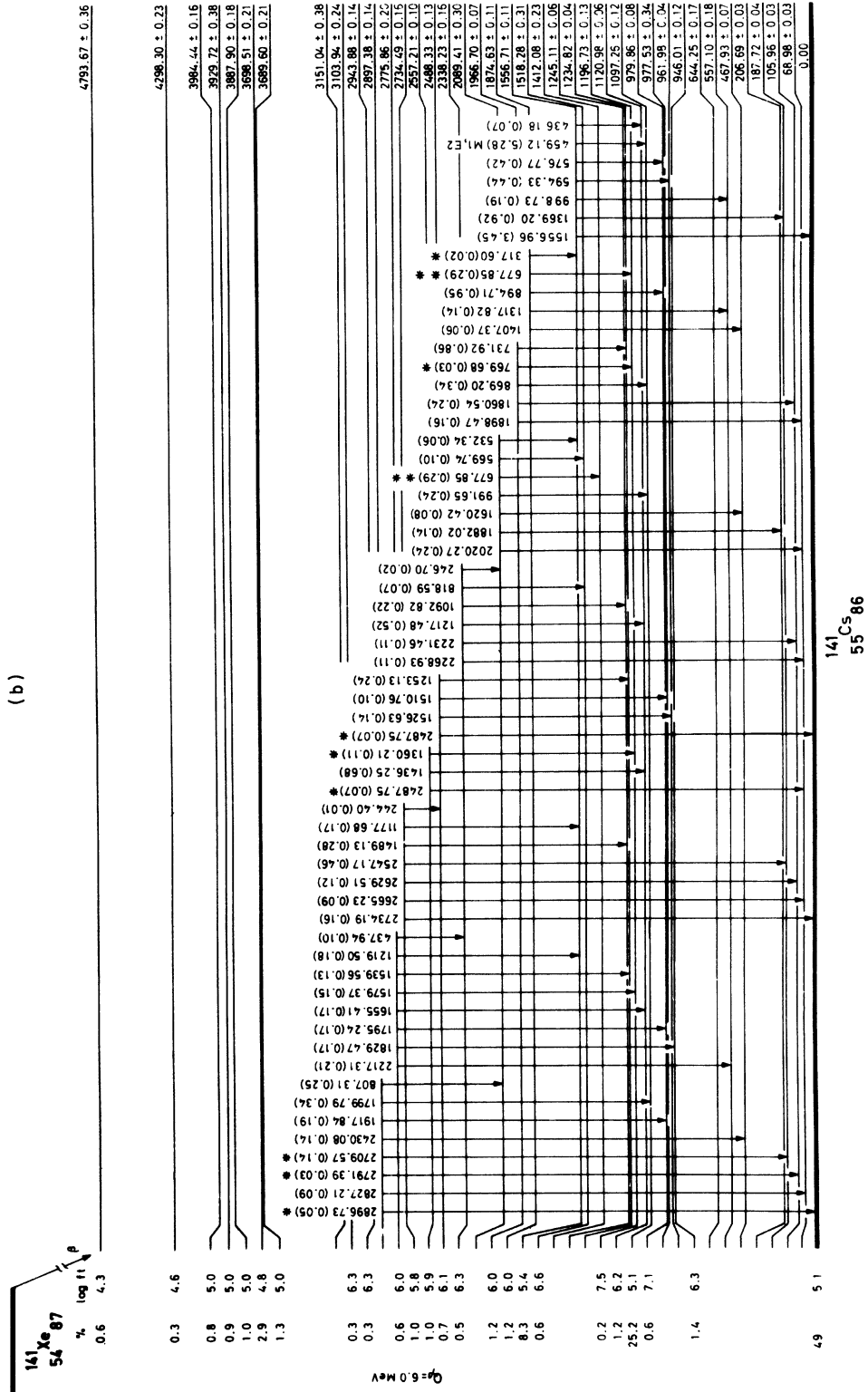 asterisks. (c) High-energy part level scheme for ^{141}Cs. Transition intensities per 100 disintegrations are given in parentheses. Doubly placed γ rays are marked with asterisks.

(b)

$^{141}_{54}Xe_{87}$
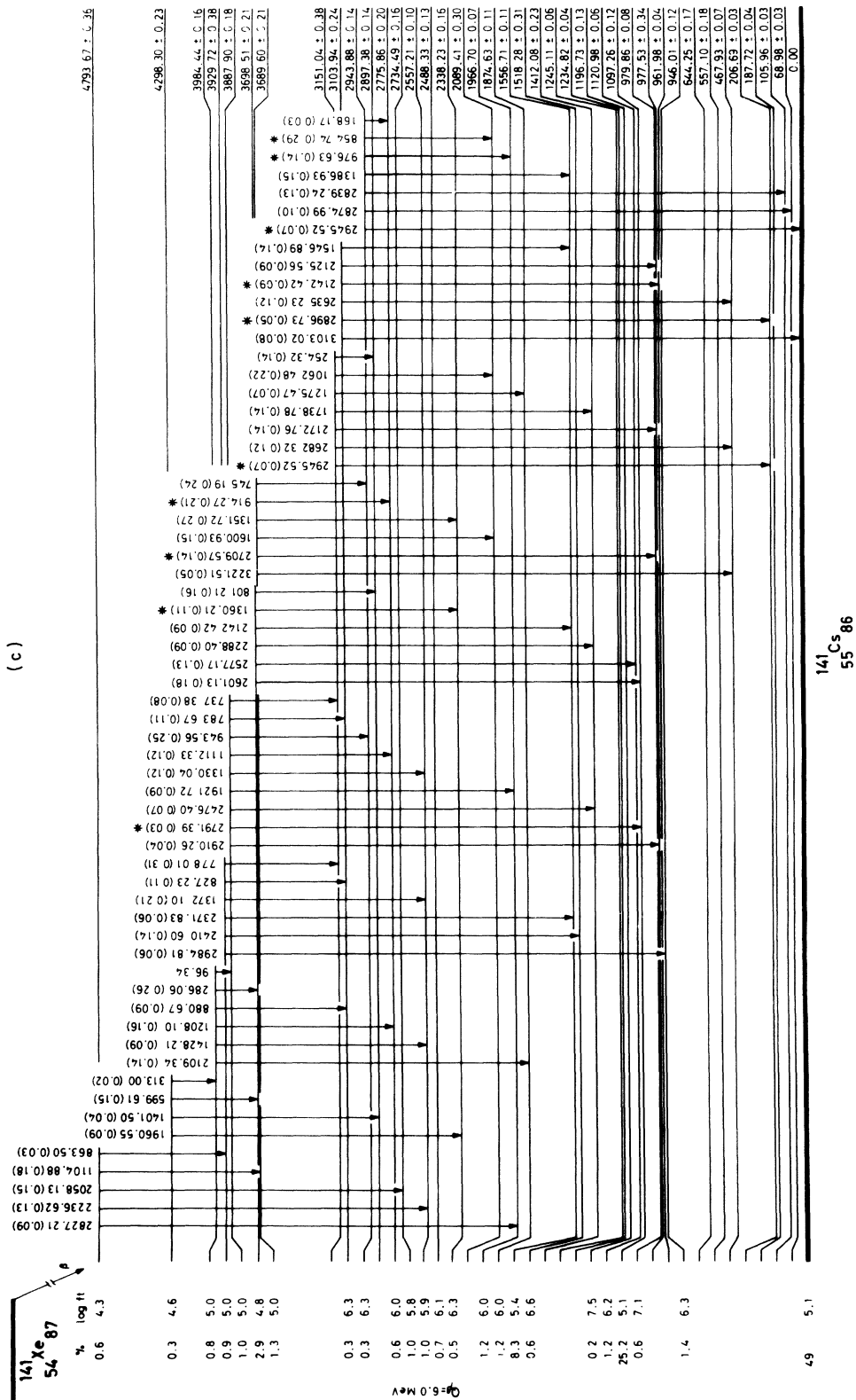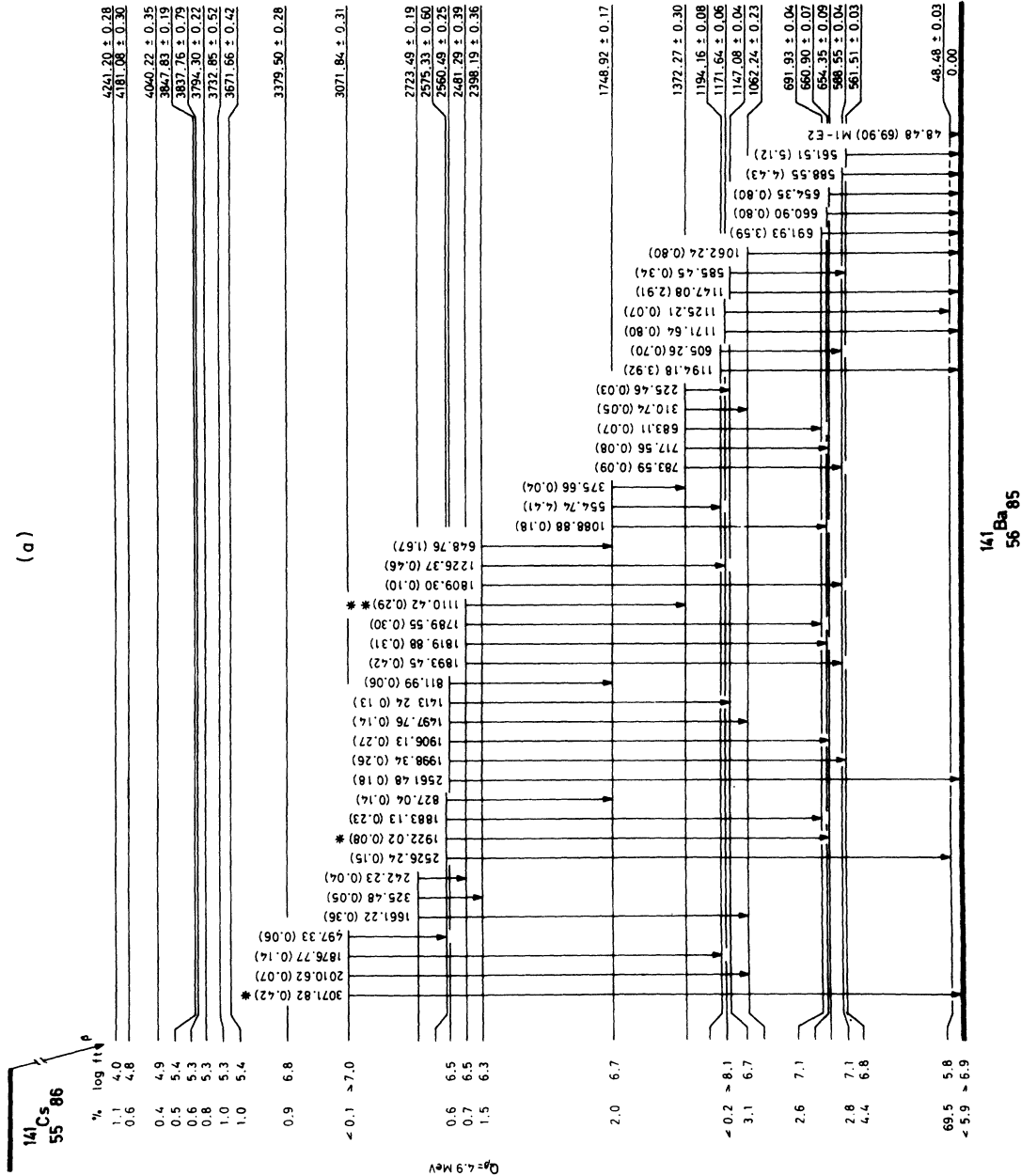
$Q_\beta = 6.0$ MeV

$^{141}_{55}Cs_{86}$

Energy levels:

4793.67 ± 0.36
4298.30 ± 0.23
3984.44 ± 0.16
3929.72 ± 0.38
3887.90 ± 0.18
3698.51 ± 0.21
3689.60 ± 0.21
3151.04 ± 0.38
3103.94 ± 0.24
2943.88 ± 0.24
2897.38 ± 0.14
2775.86 ± 0.20
2734.49 ± 0.15
2557.21 ± 0.10
2488.33 ± 0.13
2338.23 ± 0.16
2089.41 ± 0.30
1966.70 ± 0.07
1874.63 ± 0.11
1556.71 ± 0.11
1518.28 ± 0.31
1412.08 ± 0.23
1245.11 ± 0.06
1234.82 ± 0.04
1196.73 ± 0.13
1120.98 ± 0.06
1097.25 ± 0.12
979.86 ± 0.08
977.50 ± 0.34
961.98 ± 0.04
946.01 ± 0.12
644.25 ± 0.17
557.10 ± 0.18
467.93 ± 0.07
206.69 ± 0.03
187.72 ± 0.04
105.96 ± 0.03
68.98 ± 0.03
0.00

FIG. 5. (Continued)

(c)

$^{141}_{54}$Xe$_{87}$

$^{141}_{55}$Cs$_{86}$

$Q_\beta = 6.0$ MeV

FIG. 5. (Continued)

(a)

$^{141}_{55}\text{Cs}_{86}$

$^{141}_{56}\text{Ba}_{85}$

$Q_\beta = 4.9$ MeV

FIG. 6. (a) Low-energy part level scheme for ^{141}Ba. Transition intensities per 100 disintegrations are given in parentheses. Doubly placed γ rays are marked with asterisks. The percentage of β decay to each level is af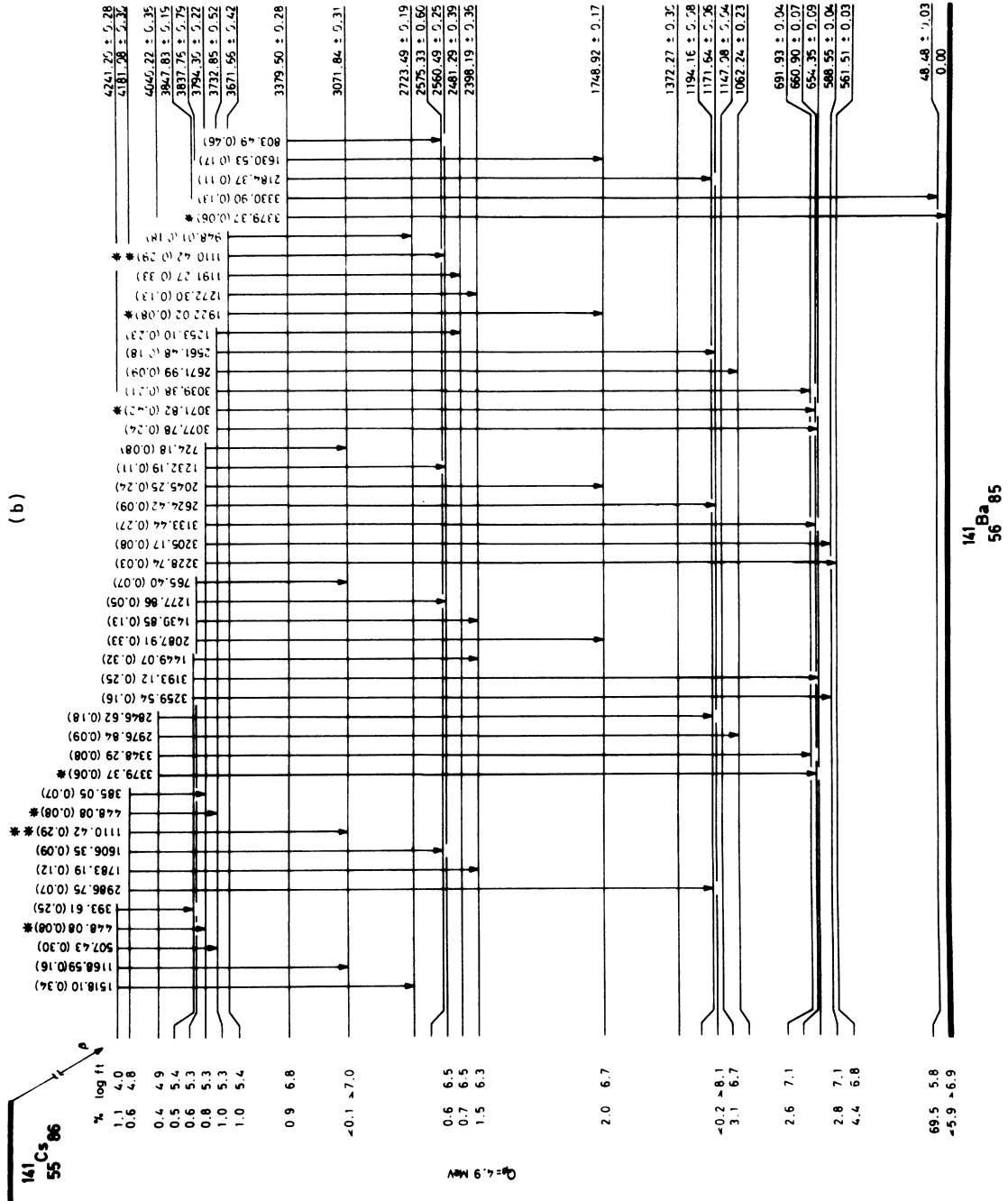fected by the error due to the unplaced γ intensity. (b) High-energy part level scheme for ^{141}Ba. Transition intensities per 100 disintegrations are given in parentheses. Doubly placed γ rays are marked with asterisks. The percentage of β decay to each level is affected by the error due to the unplaced γ intensity.

FIG. 6. *(Continued)*

[1] T. Alväger, R. A. Naumann, R. F. Petry, G. Sidenius, and T. D. Thomas, Phys. Rev. **167**, 1105 (1968).

[2] T. Tamai, J. Takada, R. Matsushita, and Y. Kiso, J. Nucl. Sci. Technol. **9**, 378 (1972).

[3] W. L. Talbert, Jr., J. W. Cook, and J. R. McConnell, private communication quoted by R. L. Auble, Nucl. Data **A10**, 175 (1973).

[4] L. Tomlinson, Nucl. Data **B12**, 179 (1973).

[5] J. A. Morman, W. C. Schick, Jr., and W. L. Talbert, Jr., Phys. Rev. C **11**, 913 (1975).

[6] E. Achterberg, F. C. Iglesias, A. E. Jech, A. Kasulín, E. Kerner, J. Mónico, J. A. Moragues, D. Otero, M. L. Pérez, M. Pinamonti, A. N. Proto, R. Requejo, J. J. Rossi, W. Scheuer, and J. F. Suarez, Nucl. Instrum. Methods **101**, 555 (1972).

[7] E. Achterberg, Ph.D. thesis (unpublished).

[8] D. Otero, Ph.D. thesis, University of La Plata, Argentina, 1974 (unpublished), [Library Dto. Física Nuclear (CNEA) No. 36 (1974)].

[9] A. N. Proto, Ph.D. thesis, University of La Plata, Argentina, 1974 (unpublished), [Library Dto. Física Nuclear (CNEA) No. 37 (1974)].

[10] E. Achterberg, F. C. Iglesias, A. E. Jech, J. A. Moragues, D. Otero, M. L. Pérez, A. N. Proto, J. J. Rossi, and W. Scheuer, Phys. Rev. C **10**, 2526 (1974).

[11] E. Achterberg, F. C. Iglesias, A. E. Jech, J. A. Moragues, D. Otero, M. L. Pérez, A. N. Proto, J. J. Rossi, W. Scheuer, and J. F. Suarez, Phys. Rev. C **5**, 1759 (1972).

[12] E. Achterberg, F. C. Iglesias, A. E. Jech, J. A. Moragues, D. Otero, M. L. Pérez, A. N. Proto, J. J. Rossi, W. Scheuer, and J. F. Suarez, Phys. Rev. C **7**, 365 (1973).

[13] R. S. Hager and E. C. Seltzer, Nucl. Data **A4**, 1 (1968).

[14] N. B. Gove, in *Nuclear Spin-Parity Assignments*, edited by N. B. Gove and R. L. Robinson (Academic, New York, 1966), p. 83.

[15] N. B. Gove and H. J. Martin, Nucl. Data **A10**, 206 (1971).

[16] J. P. Adams, G. H. Carlson, M. A. Lee, W. L. Talbert, Jr., F. K. Wohn, J. R. Clifford, and J. R. Mc Connell, Phys. Rev. C **8**, 767 (1973).

[17] K. Wünsch, H. Wollnik, and G. Siegert, Phys. Rev. C **10**, 2523 (1974).